Supporting Information

Hydricity of an Fe-H Species and Catalytic CO_2 Hydrogenation

Henry Fong and Jonas C. Peters*

Division of Chemistry and Chemical Engineering, and Joint Center for Artificial Photosynthesis, California Institute of Technology, Pasadena, CA 91125 (USA)

Contents

Methylformate Quantification 2
Catalytic Runs 3
NMR Spectra 6
IR Spectra 12
UV-vis Spectra 15
Hydricity Determination 19
UV-vis Titration 21
References 22

Methylformate Quantification

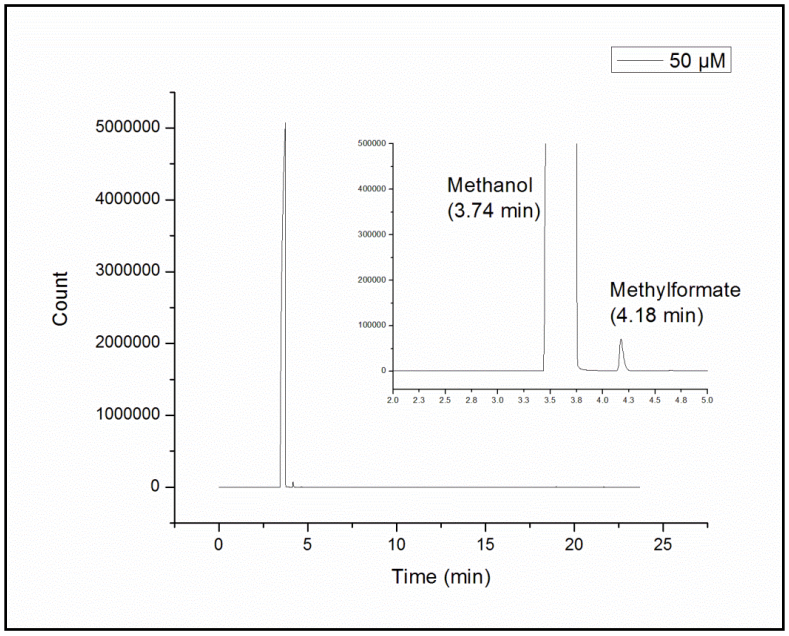

Figure S1. Example FID chromatograph of methylformate quantification. 50 µM solution of methylformate in methanol.

Catalytic Runs

Table S1. Catalytic hydrogenation results for (SiP^{R}_3)Fe, ($PhBP^{iPr}_3$)Fe, (NP^{iPr}_3)Fe, (TPB)Fe, (CP^{iPr}_3)Fe, ($C^{Si}P^{Ph}_3$)Fe, PP_3/$Fe(BF_4)_2$, and [(tetraphos)FeF](BF_4)

Entry	Precatalyst	$(Et_3NH)(OCHO)$ Yield (mmol)	MeOCHO Yield (mmol)	Total Yield (mmol)	$(Et_3NH)(OCHO)$ TON[a]	MeOCHO TON[a]	Total TON[a]	Solvent	P_{CO_2}/P_{H_2} (atm)	Additive[b]	Time (h)	Temp. (°C)
S1	(SiP^{iPr}_3)FeCl	0.00	0.00	0.00	0.00	0.00	0.00	THF	1/1		50	100
S2	(SiP^{iPr}_3)FeCl	0.00	0.00	0.00	0.00	0.00	0.00	THF	1/4		21	100
S3	(SiP^{iPr}_3)FeCl	0.00	0.00	0.00	0.00	0.00	0.00	MeOH	1/4		40	60
S4	(SiP^{iPr}_3)FeCl	0.00	0.00	0.00	0.00	0.00	0.00	THF	29/29		20	100
S5	(SiP^{iPr}_3)FeCl	0.31	0.14	0.45	39.60	18.20	57.80	MeOH	29/29		20	100
S6	(SiP^{iPr}_3)FeCl	0.31	0.13	0.44	37.90	15.30	53.20	MeOH	29/29		20	100
S7	(SiP^{iPr}_3)FeCl	0.31	0.08	0.40	37.90	10.55	48.45	MeOH	29/29		20	100
S8	(SiP^{iPr}_3)FeCl	0.14	0.00	0.14	17.40	0.00	17.40	MeOH	29/29		2	100
S9	(SiP^{iPr}_3)FeCl	0.12	0.00	0.12	15.25	0.00	15.25	MeOH	29/29		2	100
S10	(SiP^{iPr}_3)FeCl	0.26	0.10	0.35	32.54	12.20	44.74	MeOH	29/29		20	150
S11	(SiP^{iPr}_3)FeCl	0.18	0.11	0.29	22.63	13.98	36.61	MeOH	29/29		20	150
S12	(SiP^{iPr}_3)FeCl	0	0	0	0	0	0	MeOH	29/29		20	20
S13	(SiP^{iPr}_3)FeCl	0	0	0	0	0	0	MeOH	29/29		20	20
S14[c]	(SiP^{iPr}_3)FeCl	0.15	0.12	0.27	18.73	14.98	33.71	CD_3OD	29/29		20	100
S15[c]	(SiP^{iPr}_3)FeCl	0.16	0.08	0.24	19.40	10.10	29.50	CD_3OD	29/29		20	100
S16	(SiP^{iPr}_3)FeCl	0.27	0.05	0.32	34.90	6.36	41.26	MeOH	29/29	0.5 equiv $(Et_3NH)Cl$	20	100
S17	(SiP^{iPr}_3)FeCl	0.26	0.06	0.32	33.30	7.28	40.58	MeOH	29/29	0.5 equiv $(Et_3NH)Cl$	20	100
S18	(SiP^{iPr}_3)FeCl	0.68	0.15	0.83	86.31	18.90	105.21	MeOH	29/29	0.5 equiv $NaBF_4$	20	100
S19	(SiP^{iPr}_3)FeCl	0.59	0.05	0.64	75.12	6.26	81.38	MeOH	29/29	0.5 equiv $NaBF_4$	20	100
S20	(SiP^{iPr}_3)FeCl	0.31	0.28	0.59	38.1	34.6	72.7	MeOH	29/29	0.5 equiv $NaBAr^{F}_4$	20	100
S21	(SiP^{iPr}_3)FeCl	0.37	0.17	0.54	45.1	20.6	65.7	MeOH	29/29	0.5 equiv	20	100

Entry	Precatalyst	$(Et_3NH)(OCHO)$ Yield (mmol)	MeOCHO Yield (mmol)	Total Yield (mmol)	$(Et_3NH)(OCHO)$ TON[a]	MeOCHO TON[a]	Total TON[a]	Solvent	P_{CO_2}/P_{H_2} (atm)	Additive[b]	Time (h)	Temp. (°C)
										$NaBAr^F_4$		
S22	$(SiP^{iPr}_3)FeCl$	0.31	0.03	0.34	39.0	4.3	44.3	MeOH	29/29	0.5 equiv NaF	20	100
S23	$(SiP^{iPr}_3)FeCl$	0.31	0.05	0.35	39.0	6.4	45.4	MeOH	29/29	0.5 equiv NaF	20	100
S24	$(SiP^{iPr}_3)FeCl$	0.16	0.02	0.18	20.4	2.9	23.3	MeOH	29/29	0.5 equiv CsF	20	100
S25	$(SiP^{iPr}_3)FeCl$	0.19	0.02	0.21	25.0	2.9	27.9	MeOH	29/29	0.5 equiv CsF	20	100
S26[d]	$(SiP^{iPr}_3)FeCl$	0.22	0.01	0.23	28.5	1.4	29.9	MeOH	29/29	0.5 equiv TBAF	20	100
S27[d]	$(SiP^{iPr}_3)FeCl$	0.24	0.03	0.27	31.1	3.9	35.0	MeOH	29/29	0.5 equiv TBAF	20	100
S28	$(SiP^{iPr}_3)FeCl$	0.39	0.03	0.42	50.2	4.4	54.6	MeOH	29/29	0.5 equiv K_2CO_3	20	100
S29	$(SiP^{iPr}_3)FeCl$	0.45	0.01	0.46	58.3	1.7	60.0	MeOH	29/29	0.5 equiv K_2CO_3	20	100
S30	$(SiP^{iPr}_3)FeCl$	0.00	0.00	0.007	0.00	0.0	0.00	MeOH	29/0		20	100
S31	$(SiP^{iPr}_3)Fe(N_2)(H)$	0.32	0.08	0.40	41.53	9.74	51.27	MeOH	29/29		20	100
S32	$(SiP^{iPr}_3)Fe(N_2)(H)$	0.25	0.09	0.34	31.79	11.83	43.62	MeOH	29/29		20	100
S33	$(SiP^{iPr}_3)Fe(OCHO)$	0.39	0.02	0.41	51.66	2.43	54.09	MeOH	29/29		20	100
S34	$(SiP^{iPr}_3)Fe(OCHO)$	0.36	0.03	0.39	46.98	3.22	50.20	MeOH	29/29		20	100
S35	$(SiP^{Ph}_3)FeCl$	0.94	0.56	1.51	121.55	72.71	194.26	MeOH	29/29		20	100
S36	$(SiP^{Ph}_3)FeCl$	1.08	0.52	1.59	139.36	66.44	205.44	MeOH	29/29		20	100
S37	$[(SiP^{iPr}_3)Fe](BAr^F_4)$	0.10	0.03	0.13	12.72	3.82	16.54	MeOH	29/29		20	100
S38	$[(SiP^{iPr}_3)Fe](BAr^F_4)$	0.13	0.00	0.15	16.30	2.80	19.10	MeOH	29/29		20	100
S39	$(SiP^{iPr}_3)FeCl$	0.39	0.03	0.42	48.69	3.75	52.44	MeOH	29/29	Hg	20	100
S40	$(SiP^{iPr}_3)FeCl$	0.33	0.00	0.38	41.00	6.24	47.24	MeOH	29/29	Hg	20	100
S41	$HSiP^{iPr}_3/FeCl_2$ (1:1)	0.08	0.03	0.11	9.68	3.10	12.78	MeOH	29/29		20	100
S42	$HSiP^{iPr}_3/FeCl_2$ (1:1)	0.10	0.02	0.12	11.98	1.82	13.80	MeOH	29/29		20	100
S43	$(PhBP^{iPr}_3)FeCl$	0.24	0.02	0.26	29.00	3.10	32.10	MeOH	29/29		20	100

Entry	Precatalyst	$(Et_3NH)(OCHO)$ Yield (mmol)	MeOCHO Yield (mmol)	Total Yield (mmol)	$(Et_3NH)(OCHO)$ TON[a]	MeOCHO TON[a]	Total TON[a]	Solvent	P_{CO_2}/P_{H_2} (atm)	Additive[b]	Time (h)	Temp. (°C)
S44	$(PhBP^{iPr}_3)FeCl$	0.15	0.02	0.17	19.00	2.40	21.40	MeOH	29/29		20	100
S45	$[(NP^{iPr}_3)FeCl](PF_6)$	0.00	0.00	0.00	0.00	0.00	0.00	MeOH	29/29		20	100
S46	(TPB)FeCl	0.00	0.00	0.00	0.00	0.00	0.00	MeOH	29/29		20	100
S47	[(TPB)Fe] (BAr^F_4)	0.00	0.00	0.00	0.00	0.00	0.00	MeOH	29/29		20	100
S48	$(TPB)\mu\text{-}H)Fe(N_2)(H)$	0.00	0.00	0.00	0.00	0.00	0.00	MeOH	29/29		20	100
S49	$PP_3/Fe(BF_4)_2$	3.30	0.91	4.21	395.70	108.50	504.20	MeOH	29/29		20	100
S50	$PP_3/Fe(BF_4)_2$	2.69	0.98	3.67	342.24	124.68	466.92	MeOH	29/29		20	100
S51	$[(tetraphos)\text{-}Fe(F)](BF_4)$	6.06	7.68	13.74	771.30	976.50	1747.80	MeOH	29/29		20	100
S52	$[(tetraphos)\text{-}Fe(F)](BF_4)$	5.15	7.23	12.38	655.22	919.85	1575.07	MeOH	29/29		20	100
S53	$FeCl_2$	0.00	0.00	0.00	0.00	0.00	0.00	MeOH	29/29		20	100
S54	$FeCl_2$/4 PPh_3	0.00	0.00	0.00	0.00	0.00	0.00	MeOH	29/29		20	100
S55	no iron	0.00	0.00	0.00	0.00	0.00	0.00	MeOH	29/29		20	100
S56	$(SiP^{iPr}_3)Fe(N_2)(H)$	0.00	0.00	0.00	0.00	0.00	0.00	THF	1/1		20	60
S57	$(SiP^{iPr}_3)Fe(N_2)(H)$	0.00	0.00	0.00	0.00	0.00	0.00	THF	1/4		20	60
S58	$(SiP^{iPr}_3)Fe(N_2)(H)$	0.00	0.00	0.00	0.00	0.00	0.00	C_6D_6	1/4		20	90
S59	$(SiP^{iPr}_3)Fe(N_2)(H)$	0.00	0.00	0.00	0.00	0.00	0.00	THF	29/29		20	100
S60	$(SiP^{Ph}_3)Fe(N_2)(H)$	0.00	0.00	0.00	0.00	0.00	0.00	THF	29/29		20	100
S61	$(PhBP^{iPr}_3)FeCl$	0.00	0.00	0.00	0.00	0.00	0.00	THF	29/29		20	100
S62	$[(NP^{iPr}_3)Fe(N_2)(H)](PF_6)$	0.00	0.00	0.00	0.00	0.00	0.00	THF	29/29		20	100
S63	$(TPB)(\mu\text{-}H)Fe(N_2)(H)$	0.00	0.00	0.00	0.00	0.00	0.00	THF	29/29		20	100
S64	$(TPB)(\mu\text{-}H)Fe(N_2)(H)$	0.00	0.00	0.00	0.00	0.00	0.00	C_6D_6	1/4		20	100
S65	$(CP^{iPr}_3)FeCl$	0.20	0.03	0.23	24.71	3.43	28.13	MeOH	29/29		20	100
S66	$(CP^{iPr}_3)FeCl$	0.18	0.03	0.21	23.15	2.95	26.11	MeOH	29/29		20	100
S67	$(C^{Si}P^{Ph}_3)FeCl$	0	0	0	0	0	0	MeOH	29/29		20	100

Unless otherwise noted, reactions were performed under the standard conditions of 0.7 mM precatalyst, 651 mM of triethylamine, methanol (10 mL), 20 h, 100 °C, 29 atm of CO_2, and 29 atm of H_2. [a] Turnover number (TON) is the yield of product divided by the amount of added precatalyst. [c]$(Et_3NH)(OCHO)$ was detected by ^1H NMR spectroscopy, but $(Et_3ND)(OCDO)$, $(Et_3NH)(OCDO)$, and $(Et_3ND)(OCHO)$ were not detected by ^2H NMR spectroscopy. [b] BAr^F_4 = $[(3,5\text{-}(CF_3\text{-}C_6H_3)_4)B]^-$; TBAF = tetrabutylammonium fluoride.

NMR Spectra

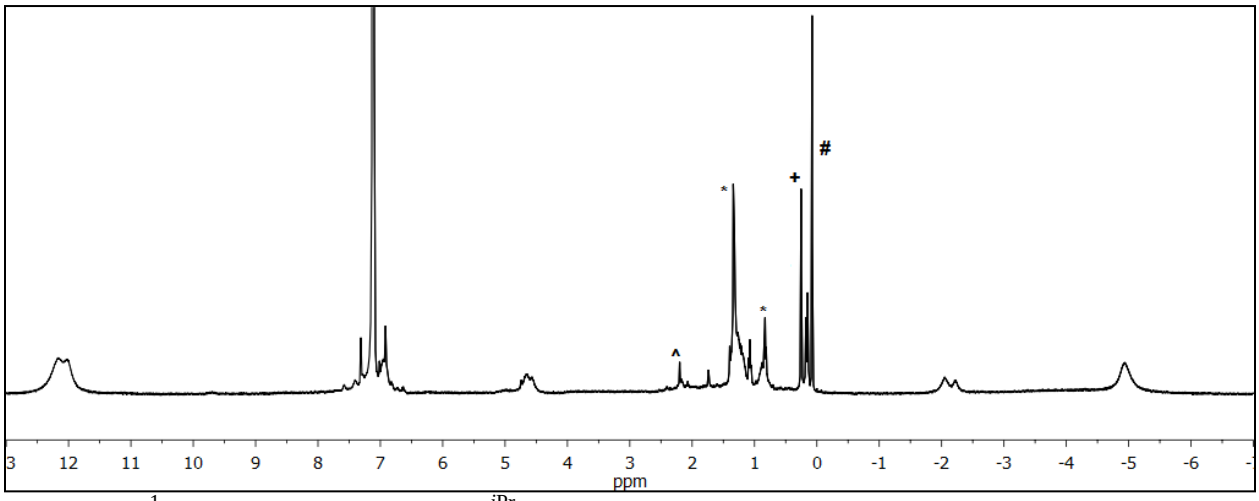

Figure S2. ^{1}H NMR spectrum of (SiP$^{iPr}_{3}$)Fe(OCHO) in C_6D_6. ^ Hexamethylbenzene, * H-grease, $^{+}$ Si-grease, $^{\#}$ HMDSO.

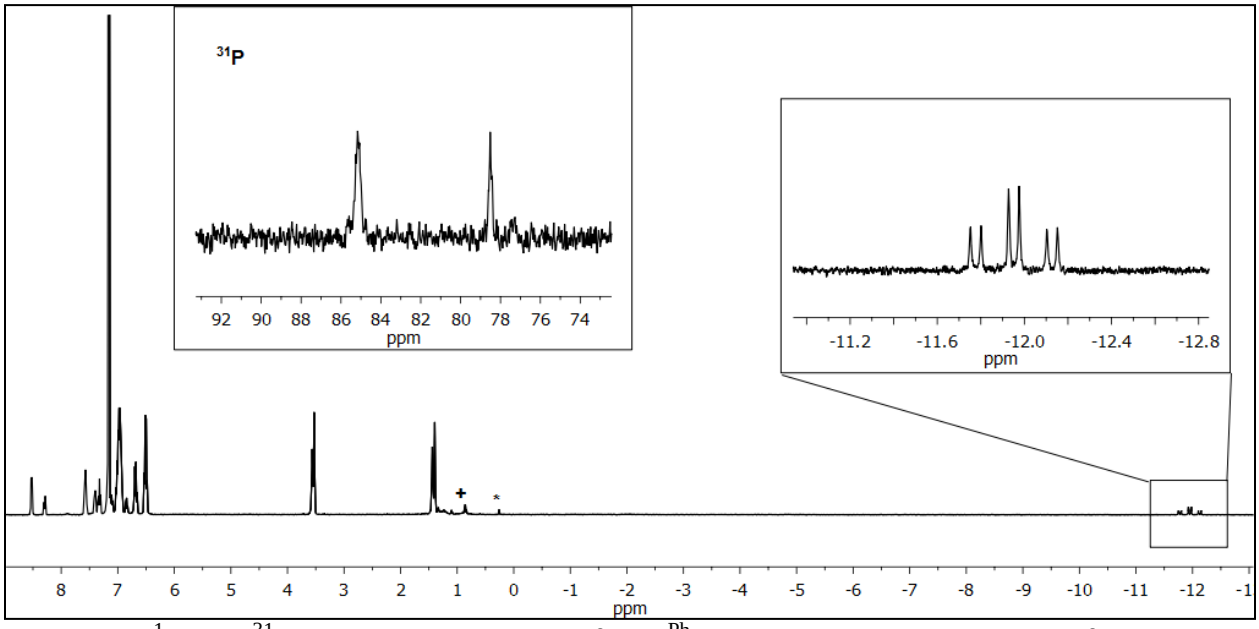

Figure S3. ^{1}H and ^{31}P (inset) NMR spectra of (SiP$^{Ph}_{3}$)Fe(N_2)(H) in a 3:2 mixture of C_6D_6:THF-d_8. $^{+}$ Si grease, * HMDSO.

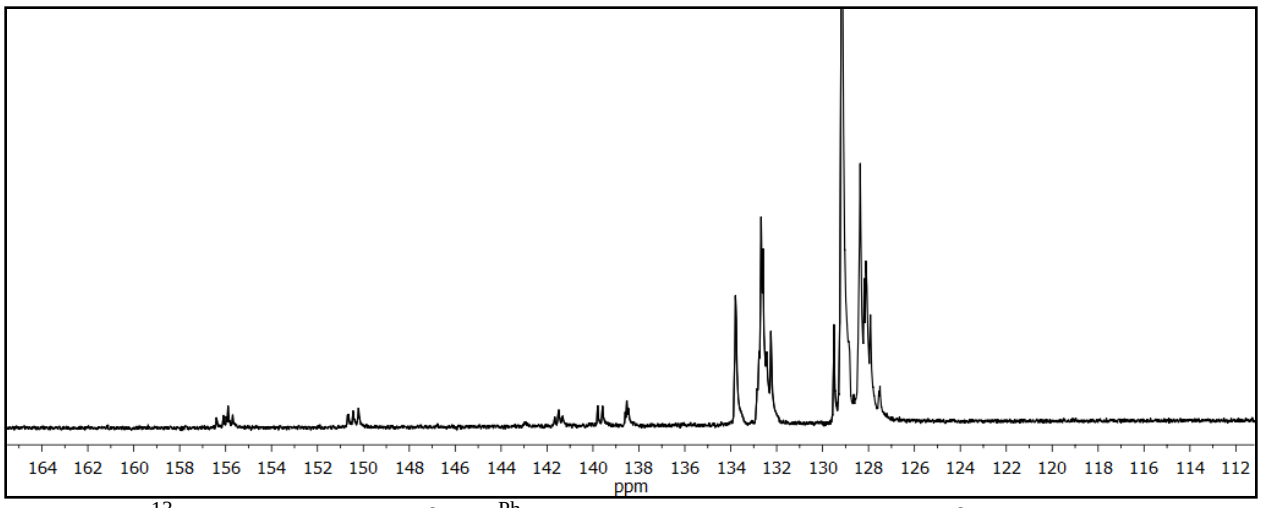

Figure S4. ^{13}C NMR spectrum of $(SiP^{Ph}_3)Fe(N_2)(H)$ in THF with a drop of C_6D_6.

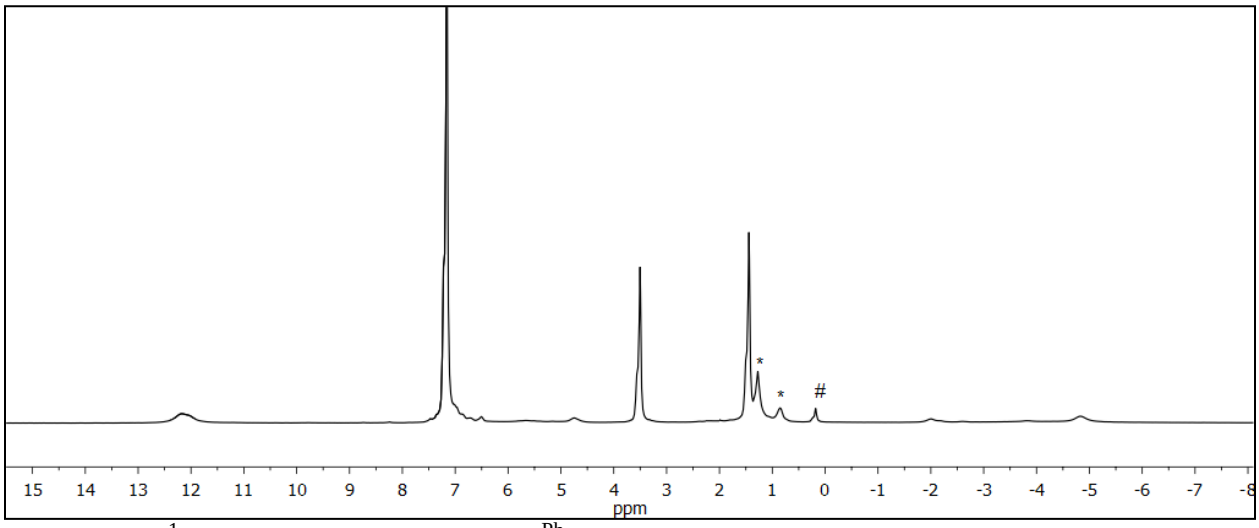

Figure S5. ^{1}H NMR spectrum of $(SiP^{Ph}_3)Fe(OCHO)$ in a 3:2 mixture of C_6D_6:THF-d_8. * Pentane, # HMDSO.

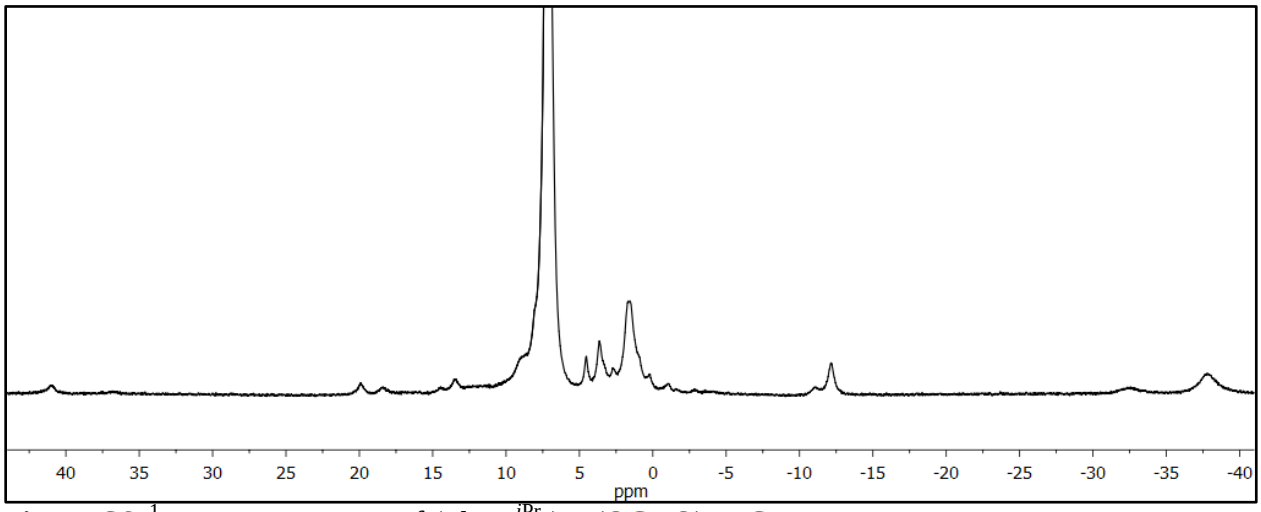

Figure S6. ^{1}H NMR spectrum of (PhBP$^{i\mathrm{Pr}}_{3}$)Fe(OCHO) in C_6D_6.

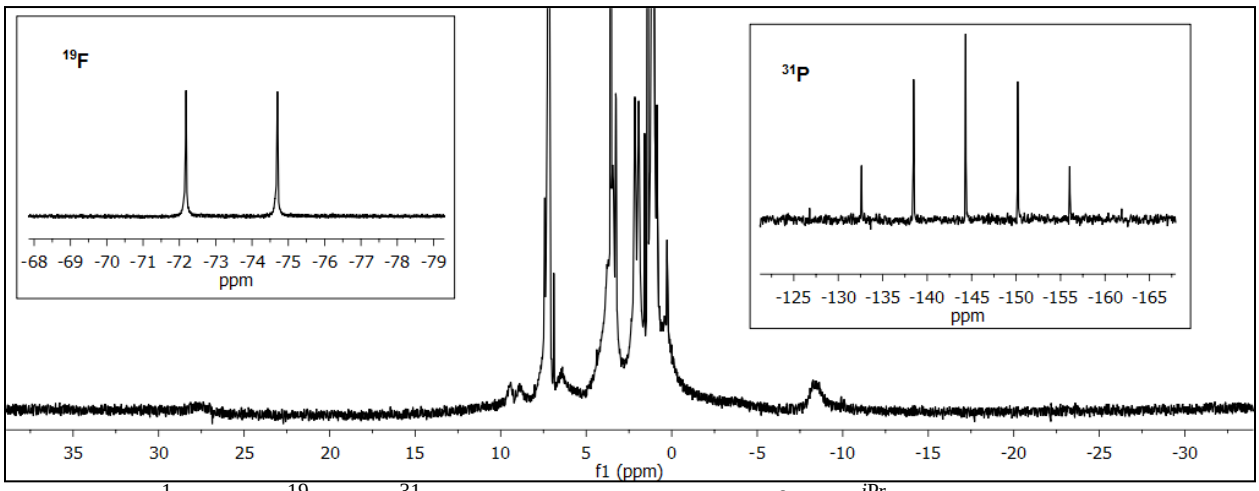

Figure S7. ^{1}H, with ^{19}F and ^{31}P (insets), NMR spectra of [(NP$^{i\mathrm{Pr}}_{3}$)Fe(OCHO)](PF$_6$) in a 3:2 mixture C_6D_6:THF-d_8.

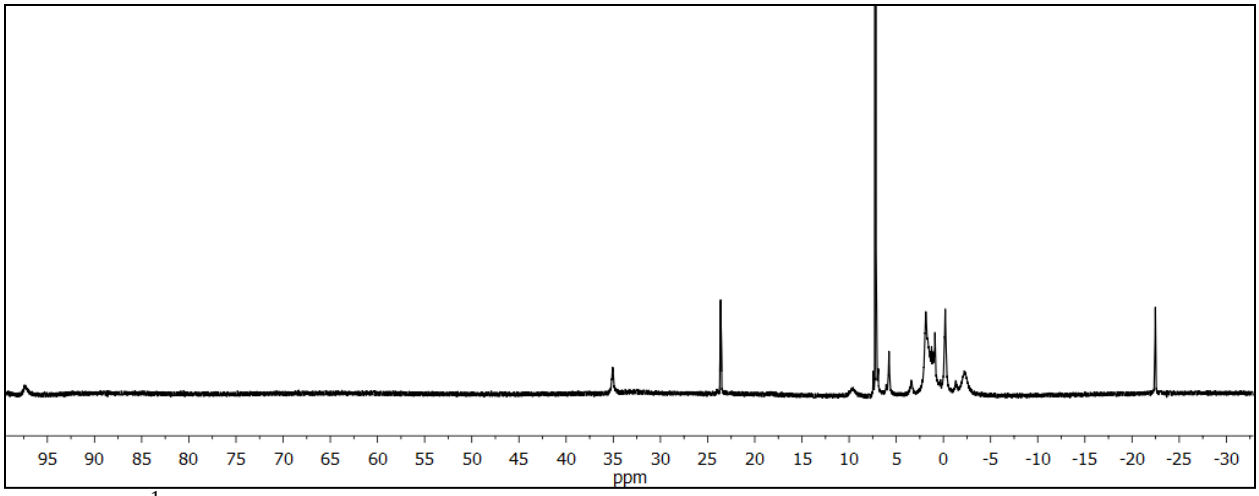

Figure S8. ^{1}H NMR spectrum of (TPB)FeCl in C_6D_6.

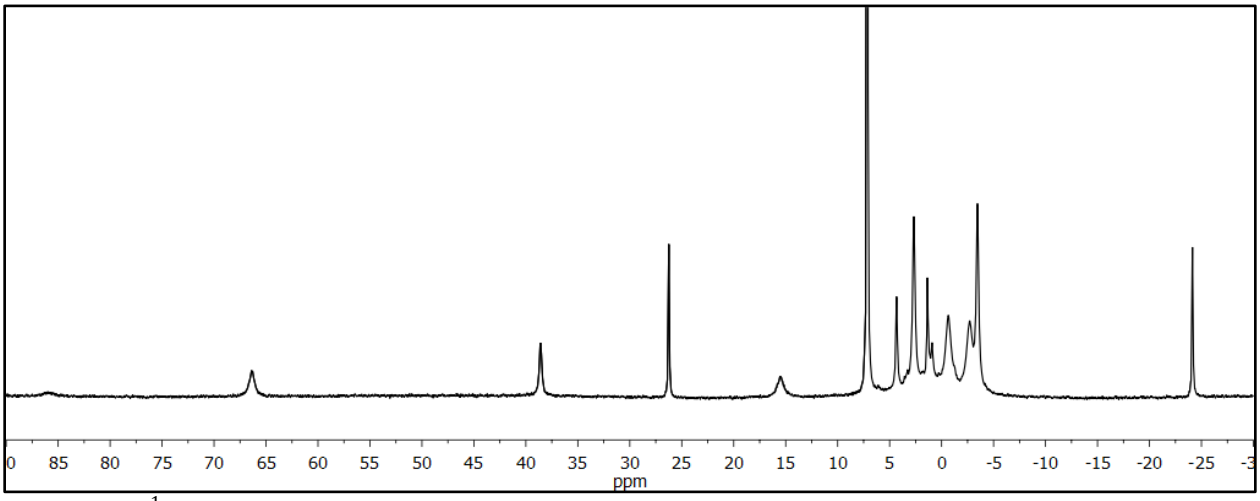

Figure S9. ^{1}H NMR spectrum of (TPB)Fe(OCHO) in C_6D_6.

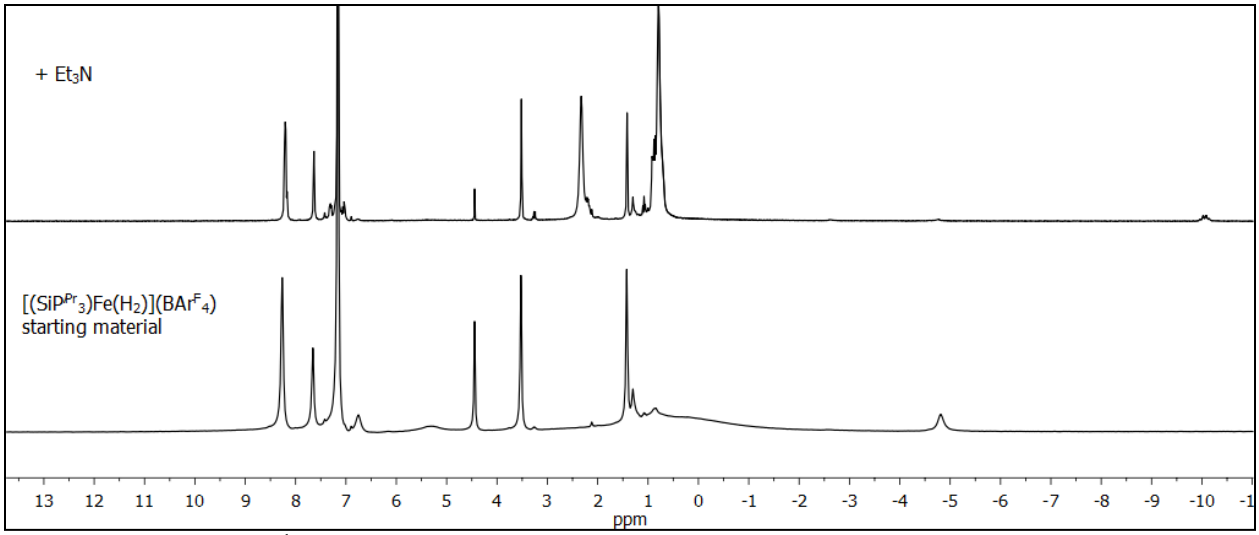

Figure S10. *In situ* ^{1}H NMR spectra in a mixture of 10:1 mixture of C_6D_6:THF-d_8 for the deprotonation of $[(SiP^{iPr}_3)(H_2)](BAr^F_4)$ by triethylamine under an H_2 atm to form $(SiP^{iPr}_3)Fe(H_2)(H)$.

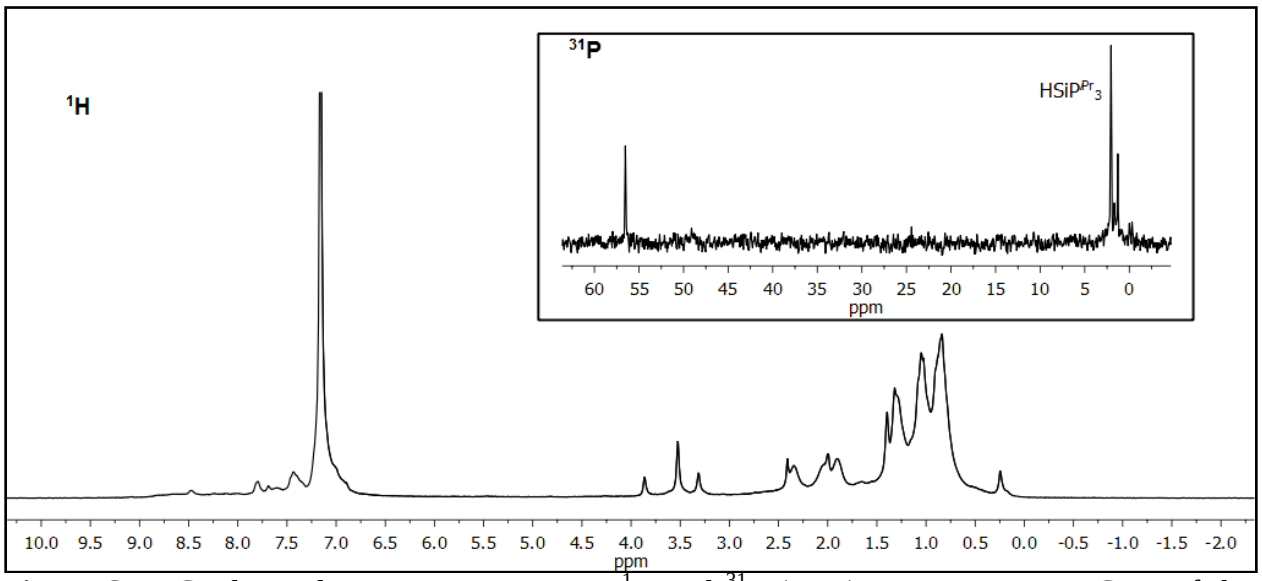

Figure S11. Crude catalytic reaction mixture. ^{1}H and ^{31}P (inset) NMR spectra in C_6D_6 of the crude catalytic reaction mixture after a high pressure catalysis experiment under standard conditions with precatalyst $(SiP^{iPr}_3)FeCl$ under the standard conditions.

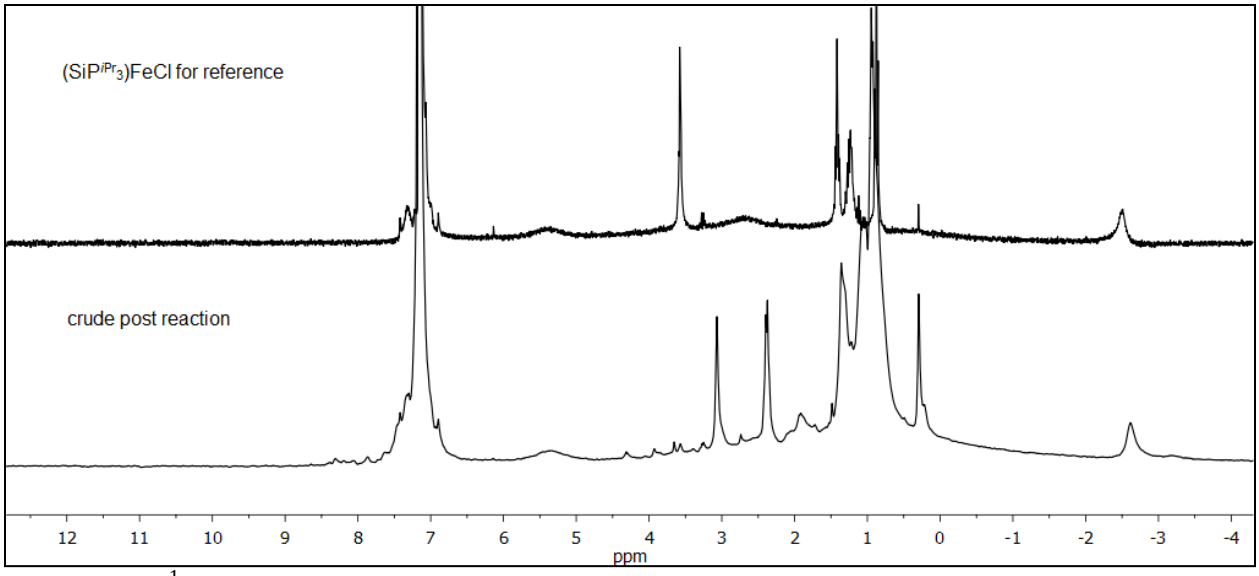

Figure S12. ^{1}H NMR spectrum in C_6D_6 of the crude, post reaction mixture after a high pressure catalysis experiment at 20 °C (bottom). The ^{1}H NMR spectrum in C_6D_6 of an authentic sample of (SiP$^{iPr}_3$)FeCl is shown for reference (top).

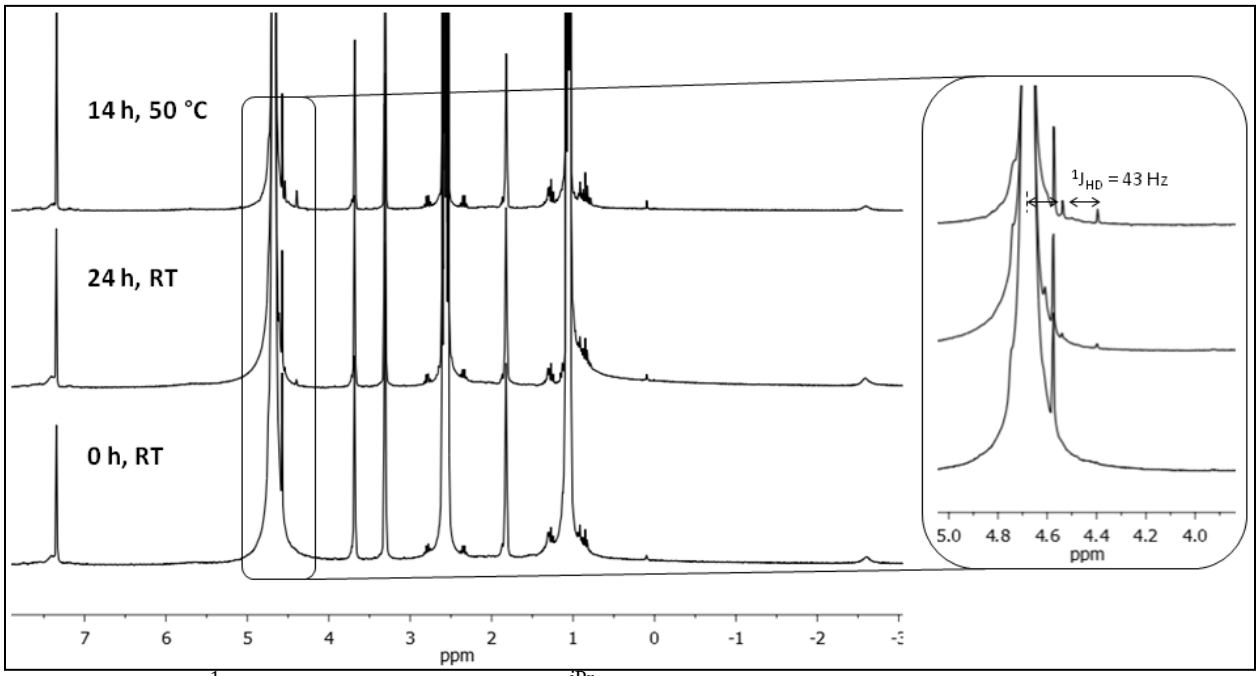

Figure S13. ^{1}H NMR spectra of (SiP$^{iPr}_3$)FeCl and excess Et_3N in a 10:1 mixture of CD_3OD:THF-d_8 under a mixture of H_2 and D_2 (1 atm:1 atm). (Bottom) At the start of the reaction (0 h) at RT, HD is not observed. (Middle) After 24 h at room temperature, a new resonance with a J_{HD} = 43 Hz is observed and corresponds to HD. (Top) After heating this reaction for 14 h at 50 °C, the signal corresponding to HD have increased relative to the middle spectrum. One peak expected at 4.68 ppm that arises from the expected 1:1:1 triplet resonance for HD is obscured by the broad H_2O signal.

IR Spectra

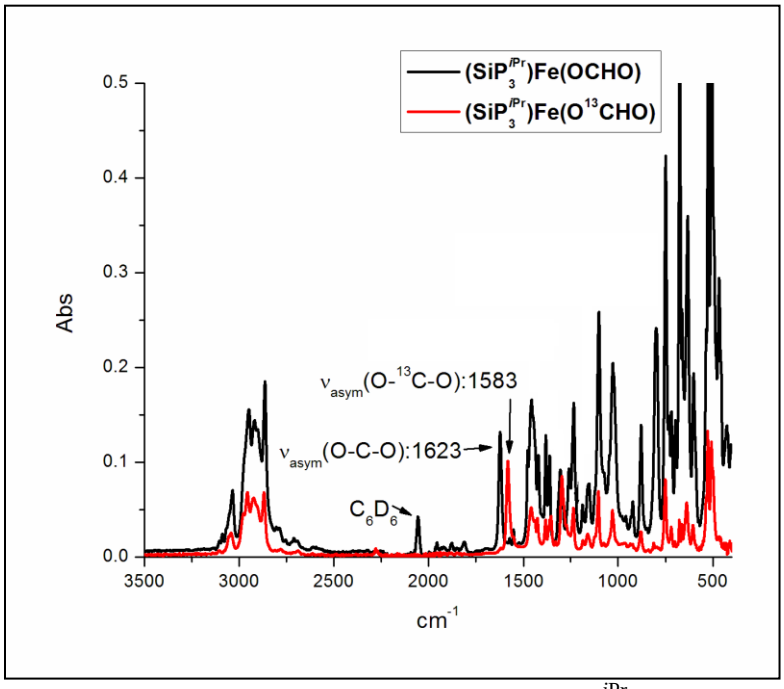

Figure S14. Thin-film ATR-IR spectra of **(**SiP$^{iPr}_3$)Fe(OCHO) and (SiP$^{iPr}_3$)Fe(O^{13}CHO).

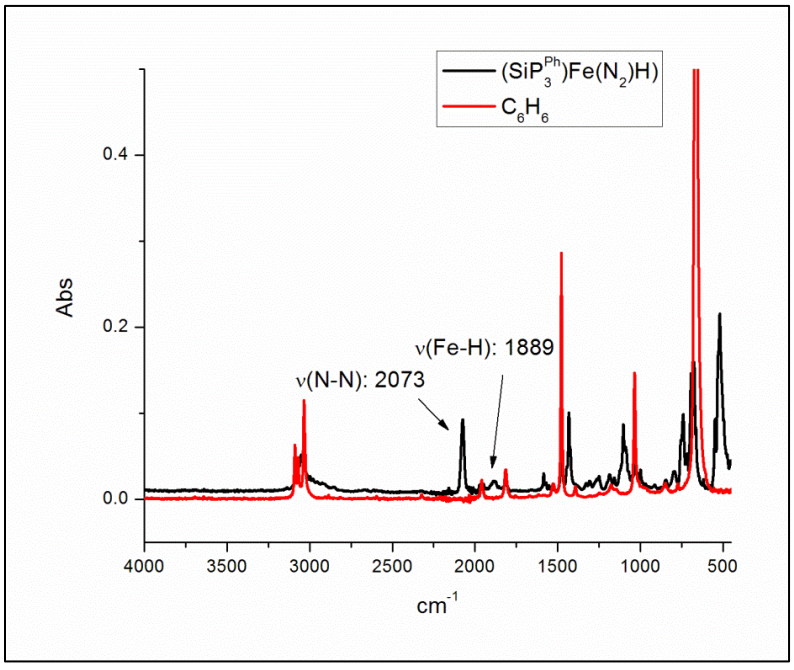

Figure S15. Thin-film ATR-IR spectrum of (SiP$^{Ph}_3$)Fe(N_2)(H) from C_6H_6 and the ATR-IR spectrum of C_6H_6 for reference.

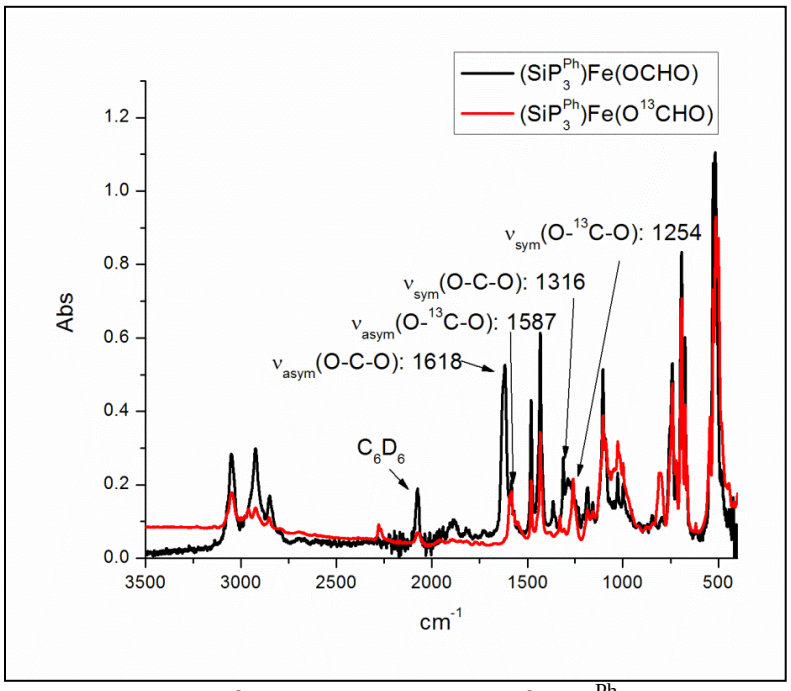

Figure S16. Thin-film ATR-IR spectra of (SiP$^{Ph}_3$)Fe(OCHO) and (SiP$^{Ph}_3$)Fe(O^{13}CHO).

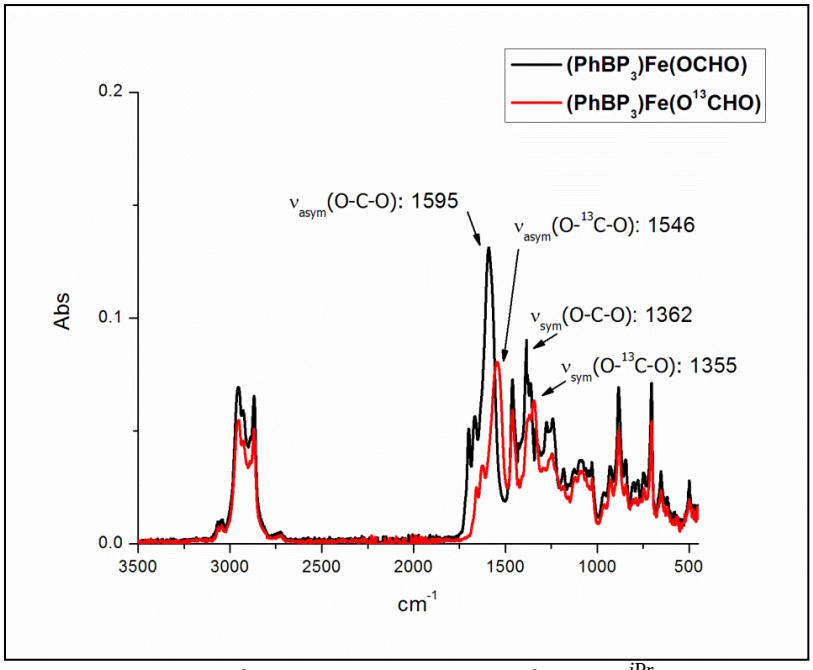

Figure S17. Thin-film ATR-IR spectra of (PhBP$^{iPr}_3$)Fe(OCHO) and (PhBP$^{iPr}_3$)Fe(O^{13}CHO).

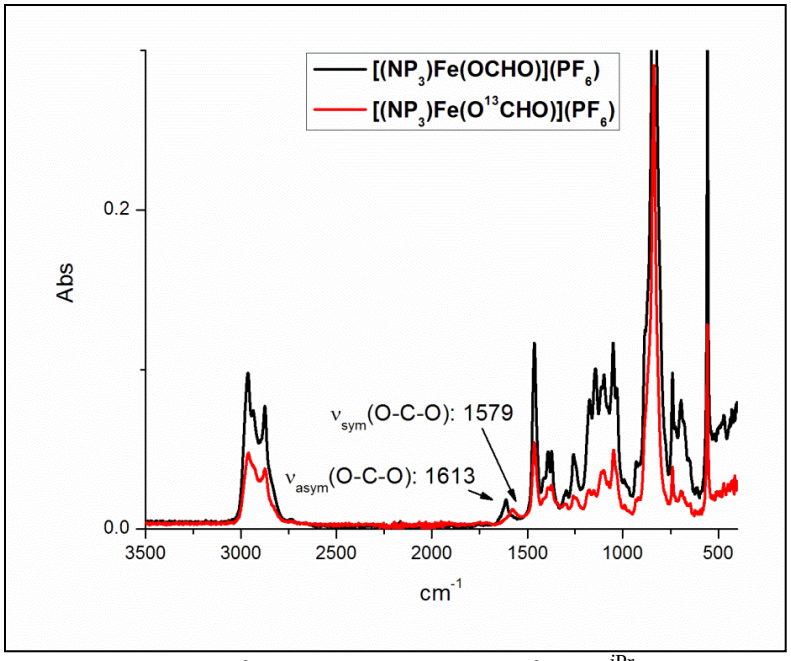

Figure S18. Thin-film ATR-IR spectra of [(NP$^{i\text{Pr}}_3$)Fe(OCHO)](PF$_6$) and [(NP$^{i\text{Pr}}_3$)Fe(O^{13}CHO).

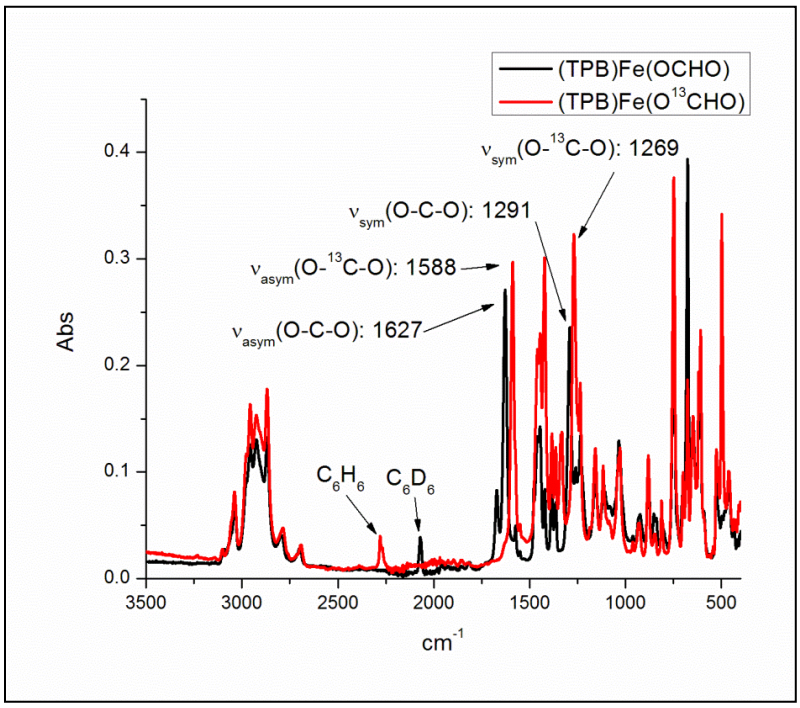

Figure S19. Thin-film ATR-IR spectra of (TPB)Fe(OCHO) and (TPB)Fe(O^{13}CHO).

UV-vis Spectra

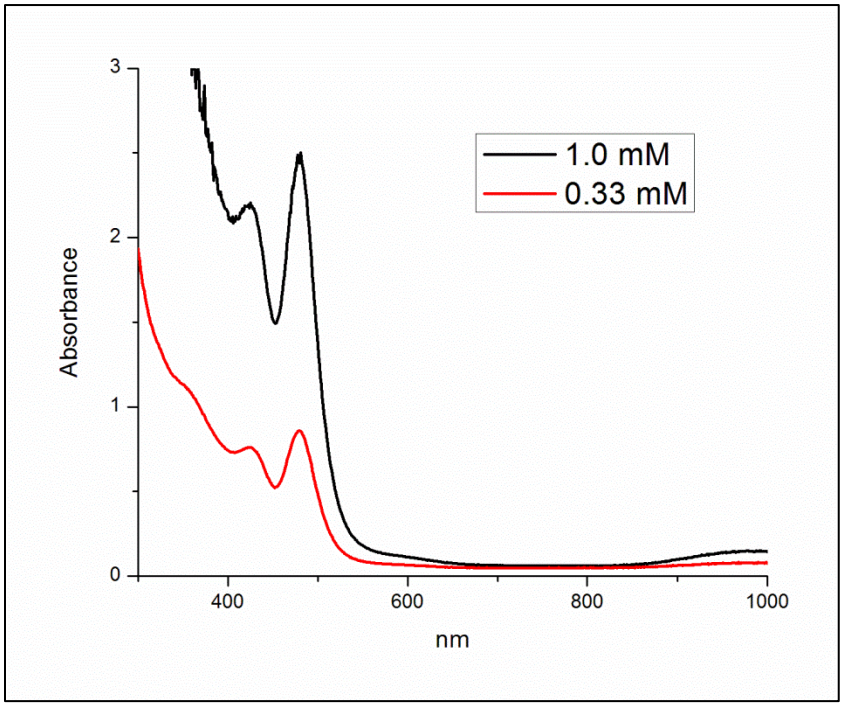

Figure S20. UV-Vis spectra of (SiP^{iPr}_3)Fe(OCHO) in THF.

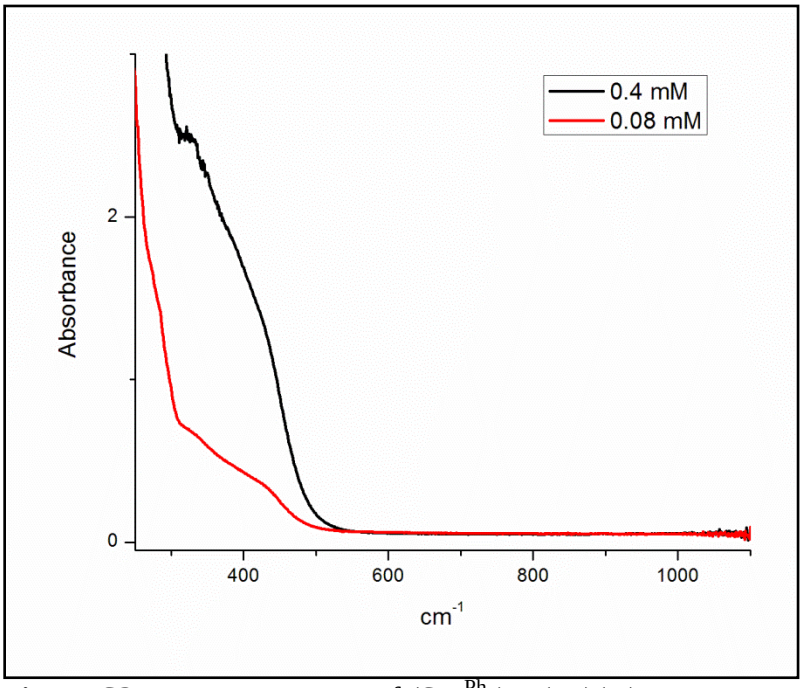

Figure S21. UV-Vis spectra of (SiP^{Ph}_3)Fe(N_2)(H) in THF.

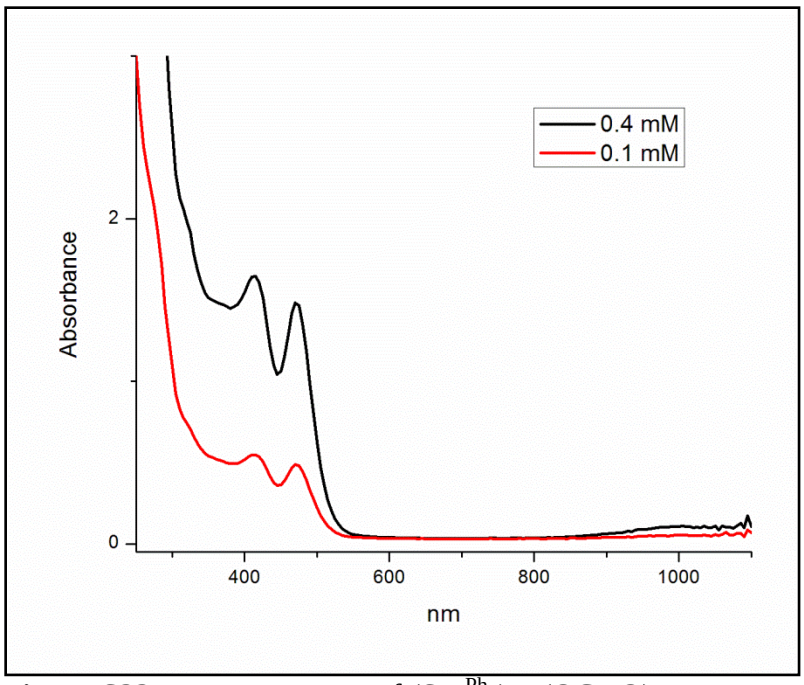

Figure S22. UV-Vis spectra of $(SiP^{Ph}_3)Fe(OCHO)$ in THF.

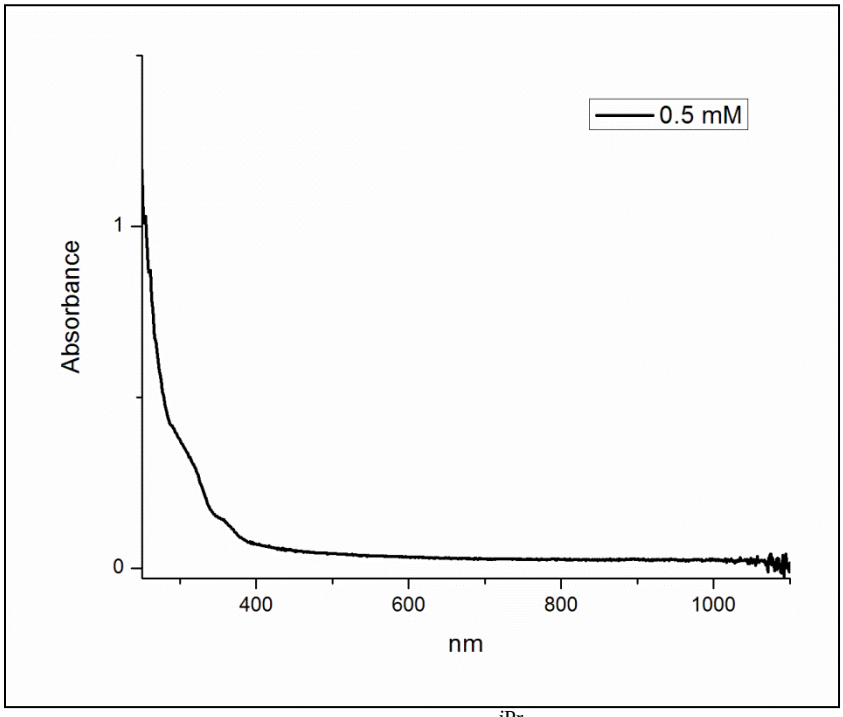

Figure S23. UV-Vis spectrum of $[(NP^{iPr}_3)Fe(OCHO)](PF_6)$ in THF.

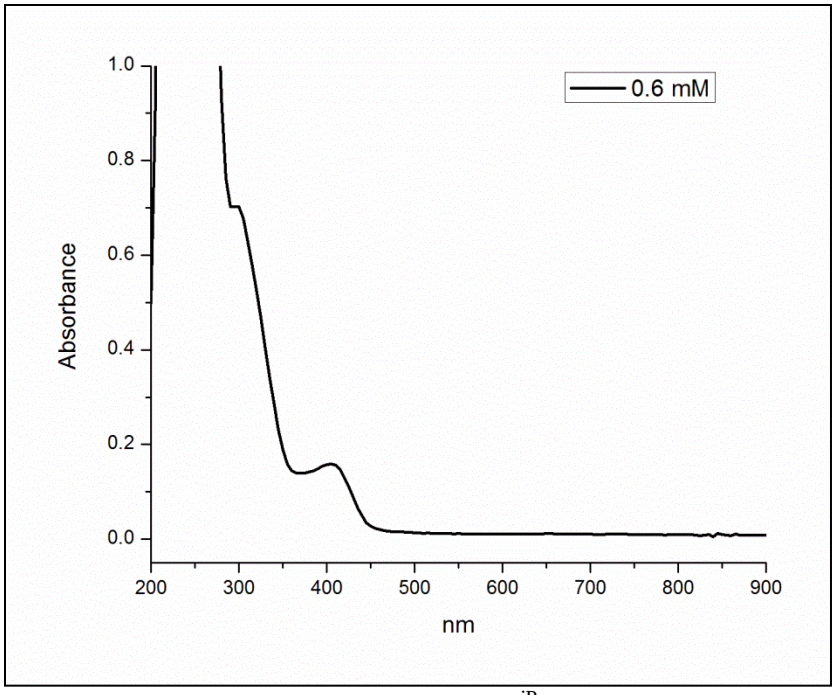

Figure S24. UV-Vis spectrum of (PhBP$^{iPr}_{3}$)Fe(OCHO) in THF.

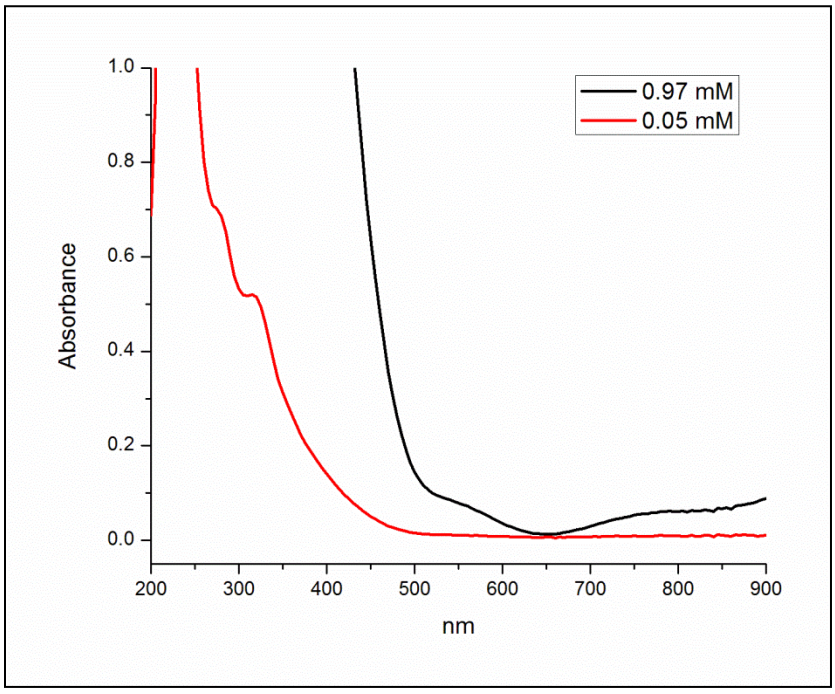

Figure S25. UV-Vis spectra of (TPB)FeCl in THF.

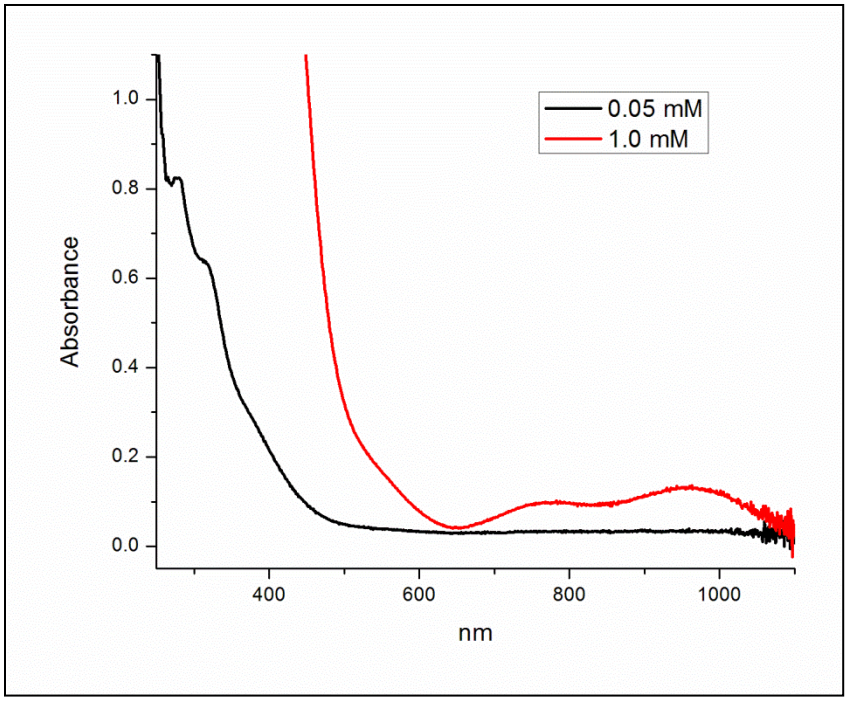

Figure S26. UV-Vis spectra of (TPB)Fe(OCHO) in THF.

Hydricity Determination

Reactions relevant to determination of hydricity for (SiP^{iPr}_3)Fe(H_2)(H) (**Fe(H_2)(H)**)with a base (B), equation S1-S3. The sum of equations S1-S3 (ΣG) represents the reverse reaction, where hydride is added to **Fe(H_2)$^+$**. Therefore, reversing the reaction and taking negative ΣG (-ΣG, equation S4) represents the hydricity (ΔG_H-) of Fe(H_2)(H).

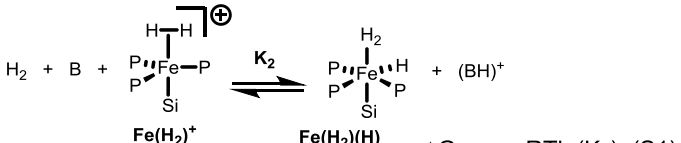

$\Delta G_{FeH} = -RT\ln(K_2)$ (S1)

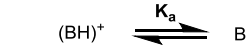

$\Delta G_{BH} = 1.364pK_a$ (S2)
or
$= -RT\ln(K_a)$

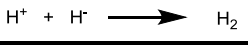

-76.0 kcal/mol (S3)

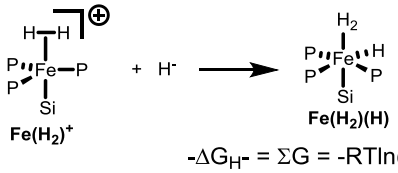

$-\Delta G_{H^-} = \Sigma G = -RT\ln(K_2) + 1.364pKa - 76.0$

or

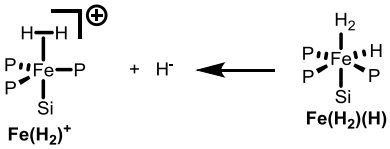

$\Delta G_{H^-} = -\Sigma G = RT\ln(K_2) - 1.364pKa + 76.0$ (S4)

Experimentally, the deprotonation reaction of equation S1 was run in THF-d_8. However, THF is known to coordinate competitively to the cationic Fe^{II} complex to give **Fe(THF)$^+$**.[1] This must be taken into account. The equilibrium constant for the competitive coordination of H_2 and THF (equation S5) has been previously reported (K_1 = 1900 M^{-1}, equation S5).

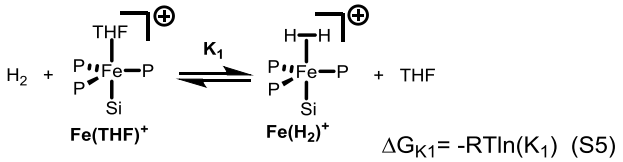

$\Delta G_{K1} = -RT\ln(K_1)$ (S5)

$$\textit{where } K_1 = \frac{[Fe(H_2)^+][THF]}{[Fe(THF)^+][H_2]} = 1900\ M^{-1}$$

Therefore, the overall reaction of equations S1 and S5 is:

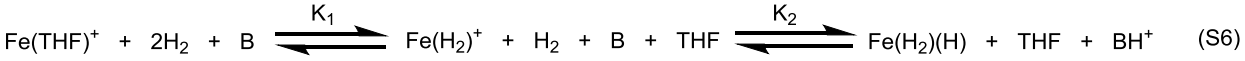

(S6)

$$\textit{where } K_2 = \frac{[Fe(H_2)(H)][BH^+]}{[Fe(H_2)^+][B][H_2]}$$

And the total concentration of iron species in solution is:

$$[Fe]_{total} = [Fe(H_2)(H)] + [Fe(H_2)^+] + [Fe(THF)^+] \quad (S7)$$

Experimentally, the equilibrium between the iron-species and base in THF-d_8 was monitored by ^{1}H NMR spectroscopy with 1,3,5-trimethoxybenzene as an integration standard. The proton resonances from the **Fe(H$_2$)(H)**, base, and conjugate acid of the base were well-resolved and reliably integrated in the ^{1}H NMR spectra, but the paramagnetic **Fe(H$_2$)$^+$** and **Fe(THF)$^+$** could not be reliably integrated. Therefore, equation S7 and K_1 were used to determine the respective concentrations of **Fe(H$_2$)$^+$** and **Fe(THF)$^+$** in order to determine the equilibrium value K_2. The activity of hydrogen at 1.0 atm was taken as unity in K_2, as this is the reference state of hydrogen for the normal hydrogen electrode.[2]

Table S2. Experimentally determined ΔG_H- for (SiP$^{i\text{Pr}}_3$)Fe(H$_2$)(H) and pK_a values for [(SiP$^{i\text{Pr}}_3$)Fe(H$_2$)](BAr$^F_4$) using three different bases.

				(SiP$^{i\text{Pr}}_3$)Fe(H$_2$)(H)	[(SiP$^{i\text{Pr}}_3$)Fe(H$_2$)](BAr$^F_4$)	
Entry	Acid	Base	K_2 (M^{-1})	ΔG_H- (kcal/mol)	pK_a^{THF}	pK_a^{MeCN}
1	[(SiP$^{i\text{Pr}}_3$)Fe(H$_2$)](BAr$^F_4$)	Proton Sponge (pK_a^{THF} = 11.1)[a]	4.31[b]	54.8	10.5	15.5
2	[(SiP$^{i\text{Pr}}_3$)Fe(H$_2$)](BAr$^F_4$)	2,6-Lutidine (pK_a^{THF} = 7.2)[a]	3.3 x 10^{-5} [c]	52.9	11.7	16.9
3	[(SiP$^{i\text{Pr}}_3$)Fe(H$_2$)](BAr$^F_4$)	2,4,6-Trimethyl-pyridine (pK_a^{THF} = 8.1)[a]	5.1 x 10^{-3} [d]	54.9	10.4	15.4
4	[Proton Sponge-H](BAr$^F_4$)	(SiP$^{i\text{Pr}}_3$)Fe(H$_2$)(H)	2.6	54.5	10.7	15.8

[a]Ref 3. [b]1 equiv of proton sponge used. [c]292 equiv of 2,6-lutidine used. [d]20 equiv of 2,4,6-trimethyl-pyridine used.

UV-vis Titration

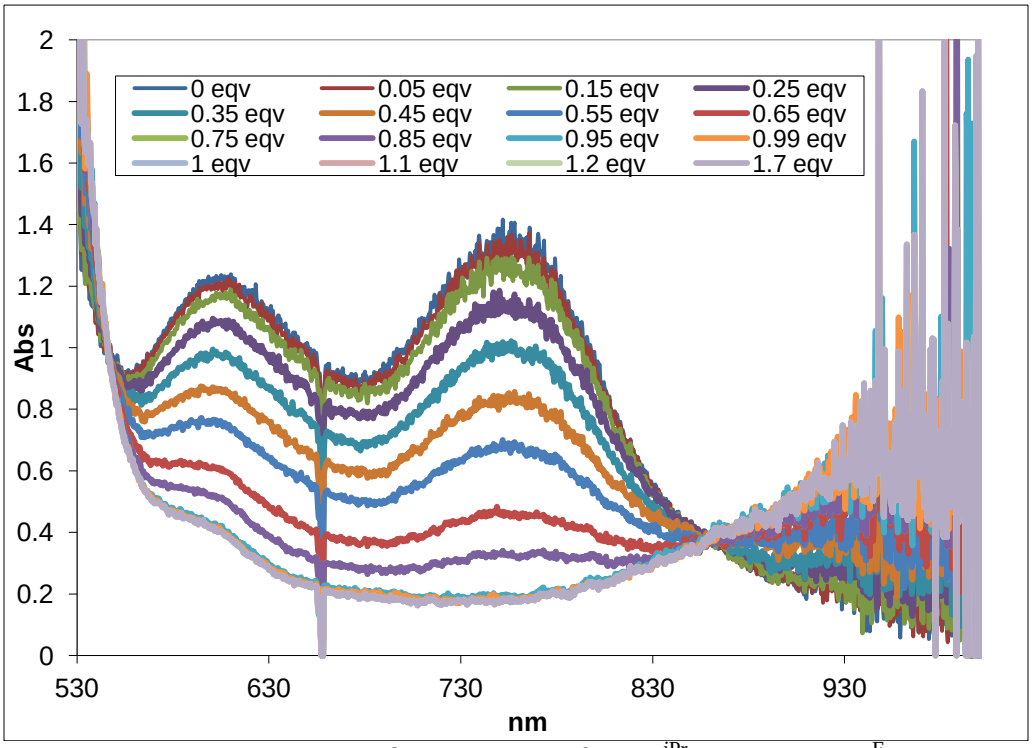

Figure S27. UV-Vis spectra of the titration of $[(SiP^{iPr}_3)Fe(N_2)](BAr^F_4)$ with Li(OCHO) in THF.

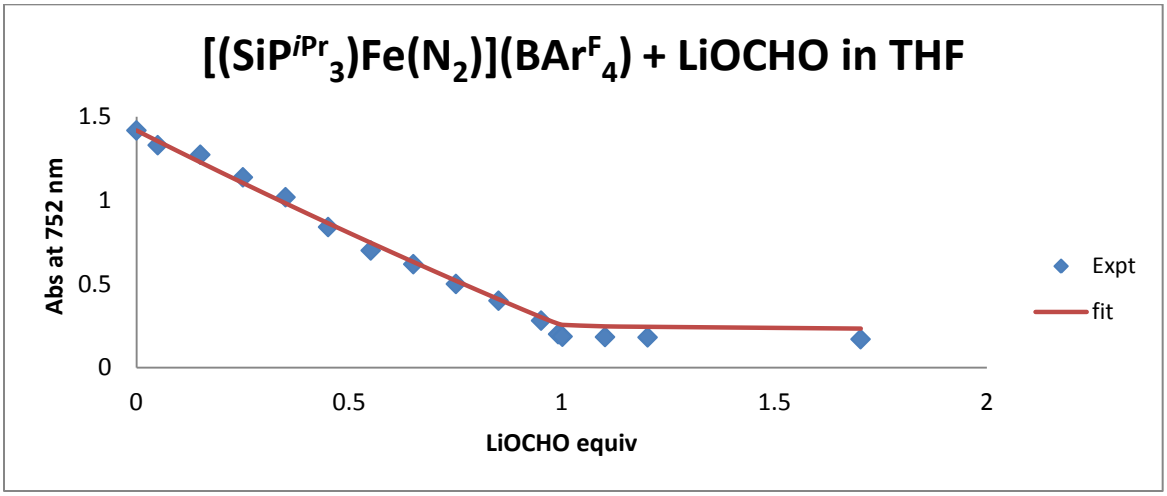

Figure S28. Absorbance at 752 nm as a function of the equivalents of Li(OCHO) added (blue diamond). The best fit of the data using $K_{eq} = 3.5 \times 10^6\ M^{-1}$ is in red.

References

1. Y. Lee, R. A. Kinney, B. M. Hoffman and J. C. Peters, *J. Am. Chem. Soc.*, 2011, **133**, 16366-16369.
2. R. Ciancanelli, B. C. Noll, D. L. DuBois and M. R. DuBois, *J. Am. Chem. Soc.*, 2002, **124**, 2984-2992.
3. I. Kaljurand, A. Kütt, L. Sooväli, T. Rodima, V. Mäemets, I. Leito and I. A. Koppel, *J. Org. Chem.*, 2005, **70**, 1019-1028.